Nath, N., Chandra, T. S., Suzuki, H., Carlos, A., & Seidel, J. C. (1982) *Biophys. J. 37*, 47a.
Okamoto, Y., & Sekine, T. (1978) *J. Biochem. (Tokyo) 83*, 1375–1379.
Okamoto, Y., & Sekine, T. (1981) *J. Biochem. (Tokyo) 89*, 697–700.
Onishi, H., & Watanabe, S. (1979) *J. Biochem. (Tokyo) 85*, 457–472.
Onishi, H., & Wakabayashi, T. (1982) *J. Biochem. (Tokyo) 92*, 871–879.
Onishi, H., & Watanabe, S. (1984) *J. Biochem. (Tokyo) 95*, 899–902.
Onishi, H., Suzuki, H., Nakamura, K., Takahashi, K., & Watanabe, S. (1978) *J. Biochem. (Tokyo) 83*, 835–847.
Onishi, H., Wakabayashi, T., Kamata, T., & Watanabe, S. (1983) *J. Biochem. (Tokyo) 94*, 1147–1154.
Persechini, A., & Hartshorne, D. J. (1983) *Biochemistry 22*, 470–476.
Seidel, J. C. (1978) *Biochem. Biophys. Res. Commun. 85*, 107–113.
Seidel, J. C. (1980) *J. Biol. Chem. 255*, 4355–4361.
Sellers, J. R., Pato, M. D., & Adelstein, R. S. (1981) *J. Biol. Chem. 256*, 13137–13142.
Sellers, J. R., Eisenberg, E., & Adelstein, R. S. (1982) *J. Biol. Chem. 257*, 13880–13883.
Sobieszek, A., & Small, J. V. (1976) *J. Mol. Biol. 102*, 75–92.
Somlyo, A. V., Butler, T. M., Bond, M., & Somlyo, A. P. (1981) *Nature (London) 294*, 567–569.
Suzuki, H., Kamata, T., Onishi, H., & Watanabe, S. (1982) *J. Biochem. (Tokyo) 91*, 1699–1705.
Stafford, W. F., III, Szentkiralyi, E. M., & Szent-Gyorgyi, A. G. (1979) *Biochemistry 18*, 5273–5280.
Trybus, K. M., Huiatt, T. W., & Lowey, S. (1982) *Proc. Natl. Acad. Sci. U.S.A. 79*, 6151–6155.
Walsh, M. P., & Hartshorne, D. J. (1982) in *Calcium and Cell Function* (Cheung, W. Y., Ed.) Vol. 3, pp 223–269, Academic Press, New York.
Walsh, M. P., Hinkins, S., Flink, I. L., & Hartshorne, D. J. (1982) *Biochemistry 21*, 6890–6896.
Walsh, M. P., Hinkins, S., Dabrowska, R., & Hartshorne, D. J. (1983) *Methods Enzymol. 99*, 279–288.

# Control of Energy Production in the Heart: A New Function for Fatty Acid Binding Protein

Nestor Clovis Fournier* and Mohammed Rahim
*Nestlé Research Department, CH-1814 La Tour-de-Peilz, Switzerland*
*Received August 13, 1984*

ABSTRACT: The quantitative subcellular distribution of the fatty acid binding protein (FABP) in heart muscle is reported for the first time. A gradient-like distribution according to the following pattern was observed: 6.96 mg·mL$^{-1}$ on the myofibrils, 2.77 mg·mL$^{-1}$ in the spaces surrounding the mitochondria, and 2.21 mg·mL$^{-1}$ in the mitochondria. This heterogeneous distribution suggests that the local in vivo concentration of FABP might fluctuate as a function of time. The consequences of these possible fluctuations, particularly in the mitochondrial vicinity, were analyzed in an in vitro system containing a fixed concentration of cardiac mitochondria and stearic acid but variable concentrations of FABP. Competition for the fatty acid was observed between the mitochondrial membranes and the binding sites on the protein. Maximal binding of fatty acid to FABP was detected in the range of FABP concentration between 1 and 3 mg·mL$^{-1}$. Remarkably, in this concentration range, two emerging peaks of $\beta$-oxidative activity were also detected. As a major conclusion, it appears that the fatty acid pool, bound to FABP, is the source of fatty acid providing the $\beta$-oxidative system with substrate. The mechanism of fatty acid transfer from this pool toward the $\beta$-oxidative system remains an open question. However, it is suggested that a gradient-like distribution of FABP in the mitochondrial vicinity leads to the coexistence of multispecies of the protein by self-aggregation. Only two of these species seem to be involved in this fatty acid transfer. As a consequence, a strong modulation of fatty acid $\beta$-oxidation rate is observed in isolated mitochondria when the concentrations of these two species are allowed to fluctuate. In conclusion, this unique cardiac fatty acid carrier, via its self-aggregation capacity and its in vivo gradient-like distribution, may act as a powerful effector in the regulation of heart energy.

A fatty acid binding protein (FABP)[1] characterized by a very high affinity for long-chain fatty acids was detected in the heart (Ockner et al., 1972). The total purification of the protein (Fournier et al., 1978) opened the door for detailed molecular studies of this novel and unique fatty acid carrier. A remarkable property of this protein soon became apparent; although the minimal molecular weight was determined to be about 12K, at least three other species coexisting at equilibrium by self-aggregation were detected by applying circular dichroism and electron spin resonance techniques (Fournier et al., 1983; Fournier & Rahim, 1983). The biological significance of the aggregation potential of the FABP species was scrutinized in a theoretical model analysis (Fournier et al., 1983). Strong modulations of membrane-bound fatty acid dependent enzyme activity were predicted for the case where one FABP species was selectively allowed to transfer fatty acids

[1] Abbreviations: FABP, fatty acid binding protein; ESR, electron spin resonance; 12-doxylstearate, 2-(10-carboxydecyl)-2-hexyl-4,4-dimethyl-3-oxyoxazolidine; EDTA, ethylenediaminetetraacetic acid disodium salt; IEF, isoelectric focusing; CoA, coenzyme A; TLC, thin-layer chromatography.

0006-2960/85/0424-2387$01.50/0 

as substrate to the membrane enzymes.

In the present study, we experimentally verified the predictions of this theoretical model. The self-aggregation property of the FABP is demonstrated to be an efficient tool in controlling the energy level delivered by the β-oxidative system catabolizing fatty acids in the cardiac mitochondria.

## Materials and Methods

*Chemicals.* The spin-label 12-doxylstearic acid was purchased from Aldrich and used as the potassium salt. Acrylamide and Serva Blau were from Serva. Pharmalyte (pH 4–6.5), gel bond film, agarose IEF, agarose A, Sephadex, and protein A (*Staphylococcus aureus*) were purchased from Pharmacia Fine Chemicals. Carbowax 20-M [poly(ethylene glycol) compound] was from Union Carbide Chemicals Co. Glutaraldehyde and the different mineral salts mentioned in this publication were from Merck. Sucrose was from Analar and bovine serum albumin (essentially fatty acid free) from Sigma. Omnifluor and 1-$^{14}$C-labeled fatty acids were from NEN, and L-carnitine was from P-L Biochemicals. $Na_2ATP$, CoA·3Li, and NAD–1Li·2$H_2O$ were from Boehringer. The standard commercial diet for the animals used in this study was number 850 containing 5.6% (w/w) lipid, from Nafag, Gossau, Switzerland. The products used for the preparation of the other diets were purchased as follows: casein (according to Hammarsten) was obtained from Merck, Germany; cellulose, sold as Solka Floc BW-100, was from Christ, Aesch, Switzerland, vitamin diet fortification mixture to which 4.1% choline bitartrate was added was from Eurobio, Paris; minerals were Salt Mix XVII from ICN, Nutritional Biochemical, Cleveland, OH; starch was from corn. The oil used was extracted from black currant seeds and obtained from Nestlé, La Tour-de-Peilz, Switzerland.

*Buffers.* Buffer A consisted of the two following solutions: (a) 0.05 M $NaH_2PO_4$·1$H_2O$ and 0.25 M sucrose; (b) 0.005 M $Na_2HPO_4$·2$H_2O$ and 0.25 M sucrose; solution a was added to solution b in order to get pH 7.4.

Buffer B was the same as buffer A but without sucrose. Furthermore, 0.02% sodium azide was added.

Buffer C contained $7.9 \times 10^{-3}$ M sodium phosphate (pH 7.4), $3.97 \times 10^{-4}$ M EDTA, $6.7 \times 10^{-2}$ M KCl, and 0.1 M sucrose.

Buffer D consisted of $1.98 \times 10^{-2}$ M Tris, 0.25 M sucrose, $2.0 \times 10^{-3}$ M EDTA, and 0.1% fatty acid free bovine albumin, final pH adjusted to 7.4 with 5 M HCl.

Buffer E was made as follows: 4 g of barbituric acid was dissolved and boiled in 100 mL of distilled water; 900 mL of distilled water was added, followed by 20.6 g of sodium barbital and 1 g of sodium azide. The resulting pH 8.4 buffer could be stored as a stock solution for months at 4 °C. Before use, this stock solution was diluted with distilled water (buffer:distilled water ratio of 1:3 v/v).

Buffer F was 0.01 M pH 7.4 sodium phosphate containing 0.01% sodium azide and 0.9% NaCl.

Buffer G consisted of buffer F plus 0.02% Carbowax 20-M [poly(ethylene glycol)]. This solution was filtered through Millipore filters (0.45-μm pore size).

*Protein Dosage.* Protein dosage was according to the Bio-Rad microassay procedure (brochure 78-0791) using acidic Coomassie Brilliant Blue reagent. Mitochondrial protein dosage was performed with the same procedure, but with a pretreatment of samples, 10 min at 60 °C in 0.4 M NaOH, as described by Gogstad & Krutnes (1982). Bovine albumin was used as standard.

*Electrophoresis.* Analytical isoelectric gels (Figure 1) were according to brochure 52-1536-01 from Pharmacia Fine Chemicals. A Pharmalyte, pH 4–6.5 range, was used. p*I*'s were determined by pH measurement of microsamples obtained by slicing the gel close to the electrophoretic bands with an LKB gel slicer system and then soaking the pieces of gel in 0.1 M KCl. The [1-$^{14}$C]palmitate radioactivity was detected on the gel (Figure 1) by scanning the latter with a Le Croy 3500 analyzer connected to an automatic TLC linear analyzer from Berthold.

*Heart Mitochondria Isolation.* Six hearts were removed from 250-g Sprague-Dawley male rats and then washed, minced with scissors, and stabilized for 30 min in buffer D at 4 °C. After homogenization (15 strokes in a Potter system) in 25 mL of buffer D and 10-min centrifugation at 4 °C and at $320g_{av}$, the supernatant was centrifuged for 10 min at $560g_{av}$; the resulting supernatant was again centrifuged for 10 min at $5100g_{av}$. The pellet was resuspended in 25 mL of buffer C and centrifuged for 10 min at $5100g_{av}$. The resulting pellet was resuspended in 0.25 mL of buffer C and centrifuged in a swing-out system for 10 min at $4200g_{av}$ in an end-closed Pasteur pipet, cut at 6 cm from the tip and immersed in a plastic tube containing water at 4 °C. The capillary part of the pipet was cut, and the mitochondria contained in this part were collected in 1 mL of buffer C. This method yielded about 2 mg of mitochondrial protein and about 98% of matrix-dense mitochondria as controlled by electron microscopy (results not shown).

*Anti-FABP Serum Production.* Two hundred fifty micrograms of totally purified FABP in 500 μL of buffer C was vortexed 5 min with 500 μL of complete Freund adjuvant and then injeced intracutaneously and bilaterally into a white rabbit (1.5 kg). A second set of injections (200 μg of FABP) was made 14 days later. A third subcutaneous injection (125 μg of FABP) was made 14 days after the second injection. Six weeks after the first injections, blood was collected from a rabbit ear vein and the serum reactivity against FABP tested on Ouchterlony plates (Miles Co.). A single precipitation line was observed. The antiserum still presented a positive reaction when collected 6 months after the start of immunization. The collected antiserum was stored at −22 °C.

*Dosage of FABP by Rocket Immunoelectrophoresis.* An agarose-containing gel was prepared by dissolving 0.35 g of agarose A in 35 mL of $H_2O$/buffer E (3:1) during 5 min at 100 °C. After the above preparation was cooled to 55 °C, 1.5 mL of rabbit antiserum (collected 3 months after the beginning of the immunization) was immediately added. The mixture was immediately pipetted between two slightly prewarmed glass plates (14 × 23 cm) separated by an interval of 1 mm width and coated on one side with a gel bond film (Pharmacia Fine Chemicals). After 5 min at room temperature and 15 min at 4 °C, the agarose gel supported on the gel bond film was separated from the two glass plates, and 4-mm diameter holes were made by suction 4 cm from the bottom; 10-μL samples to be analyzed were pipetted into the holes. These samples were from rat heart supernatant, prepared by homogenization (with a Polytron homogenizer rotating 3 min at 12000 rpm) of finely minced heart tissue in 40:1 (v/w) buffer E, followed by a 5-min centrifugation at $10700g_{av}$. Electrophoresis was performed for 4 h at 5 °C on flat-bed apparatus, FBE 3000 from Pharmacia Fine Chemicals. Initial electrical settings were 150 mA, 20 W, and 30 V. Buffer E, diluted 4 times with distilled water, was used as electrode buffer. Electrical contacts between the electrodes and the gel were obtained by using wicks purchased from Bio-rad. After a 15-min prerun, the voltage was reset at 280 V. At the end of the run, the total volt-hours was 1070. With

these conditions, the actual voltage measured on the gel surface remained constant and equivalent on the whole surface of the gel during the run. The gel was removed and dehydrated 15 min by setting on it three blotting papers (smooth surface) and a uniform weight of 500 g. After four periods of 20-min washing in 0.9% NaCl, the gel was dried with a hair dryer and colored during 12 min in the following filtered solution: 115 mL of ethanol, 181 mL of distilled water, 33 mL of acetic acid, and 1.65 g of Serva Blau. Destaining was performed by using the following solution: 100 mL of acetic acid, 350 mL of ethanol, and 550 mL of distilled water. After the gel was dried, the unknown concentrations of FABP in the sample lanes can be calculated by comparison of the rocket height with that of a series of standards of pure FABP (Figure 2).

*Fatty Acid Binding Protein (FABP) Purification.* All the operations described below were performed between 4 and 6 °C. Hearts (total weight 26 g) from Sprague-Dawley male rats, weighing 250 g, were rapidly excised, placed in buffer A, and homogenized 3 min in a Sorvall Omnimixer (position 8). After 10-min centrifugation at $5000g_{max}$ and then 60 min at $180000g_{max}$, the supernatant was delipidated according to the A procedure of Morton (1955) and then lyophilized. The resulting powder was dissolved in 24 mL of buffer A and centrifuged 30 min at $180000g_{max}$. The supernatant was gel filtered through Sephadex G-75 (7 × 50 cm) with buffer B at a flow rate of 60 mL·h$^{-1}$. Samples of 12-mL volume were collected. A first peak detectable by $OD_{280}$ measurement appeared followed by a second peak. The seven central fractions of the second peak were pooled, and the volume was reduced to 0.5 mL by ultrafiltration in an Amicon cell (YM 10 membrane). The sample was frozen and stored at −22 °C. After two of the above samples were thawed (initially corresponding to 52 g of wet heart tissue) and centrifuged for 5 min at $10700g_{max}$, the proteins contained in the supernatant (1 mL) were separated by the flat-bed agarose–Sephadex isoelectric focusing (FAS-IEF) method as described in Pharmacia Fine Chemicals Brochure (1982), using a 23 × 23 cm plate, a 5-mm-thick gel, and Pharmalyte, pH 4–6.5. The protein-containing sample was deposited 7 cm from the positive electrode. Electrophoresis took place during 4 h, with electrical presettings of 3000 V, 150 mA, and 40 W and with final volt-hours of 4180. Fractions of 0.5 cm of gel were cut, collected in 5 mL of buffer C, and left overnight at 4 °C. After vortexing and filtration of the supernatants, they were dialyzed (Spectrapor tubing molecular weight cutoff of 6000–8000) overnight against buffer C. Aliquots (300 μL) of these supernatants were concentrated to 25 μL and then processed for qualitative isoelectric focusing (Figure 1B) as described in Electrophoresis under Materials and Methods. The pure fractions (corresponding to fractions 14 and 15 in Figure 1B) were gel filtered on Sephadex G 50 superfine in buffer C. The remaining Pharmalyte was eliminated by filtration (three runs) in a 10-mL Amicon cell (membrane YM 10). The pure protein was frozen and stored at −22 °C in buffer C.

*Immunocytochemical Detection of FABP by the Protein A–Gold Method.* Three male Sprague-Dawley rats, weighing 300 g, fed ad libitum a standard commercial diet containing 5.6% (by weight) lipids, were anesthetized with Nembutal. Hearts were fixed by aortic perfusion of 0.1 M sodium phosphate (pH 7.4) containing 2% glutaraldehyde. After ventral section of the vena cava, the flow of fixative was maintained 10 min by means of a peristaltic pump (5 mL·min$^{-1}$). After five small pieces of the left ventricle of each heart were rinsed during 1 h at 4 °C with 0.1 M pH 7.4 sodium phosphate buffer, dehydration and embedding were performed at low temperature according to the method described by Carlemalm et al. (1982) and Kellenberger et al., using K4M Lowicryl. Gold particles (diameter 18 nm) were prepared essentially according to M. Horisberger (personal communication). In short, to 100 mL of boiling distilled water, strongly vortexed with a magnet, we rapidly and respectively added 1 mL of a solution containing 1% $HAuCl_4 \cdot 4H_2O$ and then 1.8 mL of a solution containing 1% trisodium citrate. The mixture was vortexed and maintained 10 min at 100 °C and then cooled 5 min in tap water; 1.3 mL of 0.1 M $K_2CO_3$ was finally added to give pH 7.0. The binding of protein A to the gold particles was performed in a siliconized beaker after 1 mg of protein A was dissolved in 0.2 mL of distilled water, and then 10 mL of gold particle suspension prepared as above was added. After 2 min of vortexing, 0.2 mL of a solution containing 1% Carbowax 20-M was added; 8 mL of the resulting suspension was centrifuged 1 h at 60000*g* at 4 °C. The pellet was resuspended in 8 mL of buffer G. This suspension (protein A–$Au_{18}$) was kept at 4 °C. Thin sections of heart tissue collected on copper grids were marked as follows. The sections were first treated for 5 min with a solution containing 1% bovine albumin (essentially fatty acid free) in buffer F and then for 30 min with a solution containing anti-FABP serum diluted 1:50 with buffer F. After being generously rinsed in buffer F, the sections were treated, for 30 min, with the protein A–$Au_{18}$ suspension described above. After the sections were generously rinsed with buffer F and then distilled water, they were dried for 30 min at room temperature. They were then contrasted for 2 min in an aqueous solution containing 2% uranyl acetate. After the sections were rinsed with distilled water and dried for 10 min at room temperature, they were again contrasted for 1 min with lead citrate according to Reynolds (1963). Electron micrographs of 20 fields per heart, obtained after section of 5 embedded blocks per heart, were examined with a Philips EM 300 electron microscope and then enlarged to a magnification of 56000×. After numeration of gold particles on 60 micrographs representing three rat hearts, the areas of respective cell compartments were determined by using the digital planimeter MOP-10 from Kontron.

*β-Oxidation Rate Measurements.* The following initial stock solutions were prepared in buffer C: (a) $4 \times 10^{-5}$ M L-malate, $4 \times 10^{-3}$ M ATP, $3.2 \times 10^{-4}$ M CoA, $10^{-2}$ M NAD, and $2 \times 10^{-2}$ M $MgCl_2$; (a′) same as (a) but omitting CoA and adding $8 \times 10^{-3}$ M L-carnitine; (b) isolated cardiac mitochondria (0.5 mg of protein mL$^{-1}$); (c) 61.2 μM 12-doxylstearate or stearate (potassium salt) plus 2 μCi of [1-$^{14}$C]-stearate (56 mCi·mmol$^{-1}$); (d) variable concentrations of purified FABP.

The above stock solutions (a–d) kept at 4 °C (except stock c which was at room temperature) were mixed according to the following pattern at room temperature: (1) 5 μL of (b) plus 5 μL of (a); (2) 5 μL of (b) plus 5 μL of (a′); (3) 15 μL of (c) plus 15 μL of (d). After 4 min at room temperature, the following samples were prepared: (4) 10 μL of (3) put in (1); (5) 10 μL of (3) put in (2). After 1.5-min equilibration at 37 °C, 15 μL of (4) was mixed with 15 μL of (5). In this operation, the β-oxidation process was thus started by the simultaneous presence of CoA and carnitine in the incubation medium, but without any change of FABP concentration. After 2-min incubation at 37 °C, the reaction was stopped by the addition of concentrated KOH. After 30-min saponification at 70 °C in a 90% ethanol solution containing 10% KOH, the samples were acidified with concentrated HCl, and fatty acids were extracted with petroleum ether. Radioactivity was determined after solubilization of fatty acid dried extracts

Table I: Diet Compositions

| | oil | | starch | | casein | | cellulose | | vitamins | | mineral salts | |
|---|---|---|---|---|---|---|---|---|---|---|---|---|
| diet | wt % | mg·kcal$^{-1}$ | wt % | mg·kcal$^{-1}$ | wt % | mg·kcal$^{-1}$ | wt % | mg·kcal$^{-1}$ | wt % | mg·kcal$^{-1}$ | wt % | mg·kcal$^{-1}$ |
| $R_0$ | 0 | 0 | 76.36 | 212 | 13.63 | 37.9 | 3.75 | 10.4 | 1.25 | 3.5 | 5 | 13.9 |
| $R_{10}$ | 10 | 24.7 | 63.44 | 156 | 15.34 | id[a] | 4.21 | id | 1.4 | id | 5.62 | id |
| $R_{19}$ | 19 | 42.6 | 51.87 | 116 | 16.9 | id | 4.58 | id | 1.53 | id | 6.1 | id |
| $R_{38}$ | 38 | 71.4 | 27.37 | 51.4 | 20.17 | id | 5.4 | id | 1.8 | id | 7.2 | id |

[a] id means identical with the first-mentioned value.

with toluene containing 0.4% Omnifluor. The amount of $\beta$-oxidized fatty acid was determined by subtracting the radioactivity value of a nonincubated control sample from that of the incubated test samples.

*ESR Spectroscopy.* The binding capacity of 12-doxylstearic acid to FABP (Figure 7) or to the mitochondria (Figure 6) was determined quantitatively by ESR according to Fournier et al. (1983) and Hsia et al. (1973) at 37 ± 1 °C. The spectra were recorded on a Varian E line spectrometer (X band) using 100-kHz field modulation.

*Computer Analysis.* The computer operations were carried out on a Hewlet-Packard 3000 computer. The theoretical curves were fitted to the experimental points in Figures 6 and 7 by nonlinear regression.

## Results

*In Vivo FABP Content in Rat Heart and Control by Diet.* Although FABP has been detected (Ockner et al., 1972) and then purified (Fournier et al., 1978), no data are available concerning the total content of this protein in the heart and also concerning factors controlling its turnover. The experiments described in this section have been aimed at these questions.

After purification of FABP from rat heart (Figure 1) and antibody production, the quantitative dosage of the protein in the heart by the rocket immunoelectrophoresis method was determined (Figure 2). For normal adult male rats (250 g), fed ad libitum a standard commercial diet (5.6 wt % lipids), the FABP concentration was found to be 4.3 ± 0.23 mg per gram of wet heart tissue.

The dietetic factors that could alter this concentration were next investigated. For this purpose, male rats, initially weighing 200 g, were fed, for 10 days ad libitum, the oil-free $R_0$ diet described in Table I. They were then transferred for 31 days to the oil-containing diets $R_{10}$, $R_{19}$, and $R_{38}$ or remained on the $R_0$ diet (Table I). Hearts were removed, as a function of time, and processed for FABP dosage by rocket immunoelectrophoresis as described under Materials and Methods. An increasing induction of FABP synthesis was observed (Figure 3) with the following pattern: $R_{38} > R_{19} > R_{10} > R_0$.

This induction is attributable to the increasing content of oil in the diets. In fact, the diets were balanced, so that the contents of the different compounds, expressed in milligrams per kilocalorie, were identical in the four diets (Table I); only oil and starch contents were allowed to vary. The energy intake after 31 days was remarkably identical in the $R_0$, $R_{10}$, and $R_{19}$ diets; the observed values were 2097, 2010, and 2040 kcal, respectively. This means that the respective intakes of casein, cellulose, vitamins, and mineral salts, expressed in milligrams, were identical in the three considered diets and thus can be excluded as factors stimulating FABP synthesis. Starch can also be excluded since a negative correlation was observed between its content in the diets (Table I) and the stimulation of FABP synthesis. Only the oil content showed a positive correlation (Figure 3). This conclusion was cor-

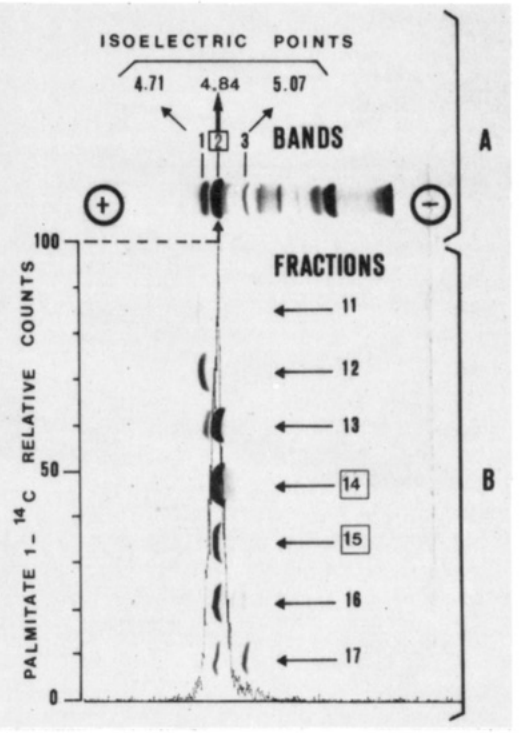


FIGURE 1: Purification of FABP from rat hearts. (A) Detection of FABP after partial purification by G-75 Sephadex gel filtration of heart supernatant as described under Materials and Methods. An aliquot (294 $\mu$g of protein) from the second $OD_{280}$ peak was electrofocused, concomitantly with 11 × $10^4$ cpm of potassium [1-$^{14}$C]palmitate, in an agarose gel containing Pharmalyte, pH 4–6.5. FABP was assigned to band 2 ($pI$ = 4.84) after the detection of the single radioactive [1-$^{14}$C]palmitate signal centered on this band. (B) Total purification (fractions 14–15) of FABP by quantitative flatbed agarose–Sephadex isoelectric focusing of 29.4 mg of protein, taken from the second peak ($OD_{280}$), obtained after G-75 Sephadex gel filtration of heart supernatant as described under Materials and Methods. The B gel represents the analytical isoelectric focusing pattern of aliquots of the different fractions obtained after slicing the quantitative gel into parts of 5 mm. The numbering started from the positive electrode. Both A and B gels were run concomitantly.

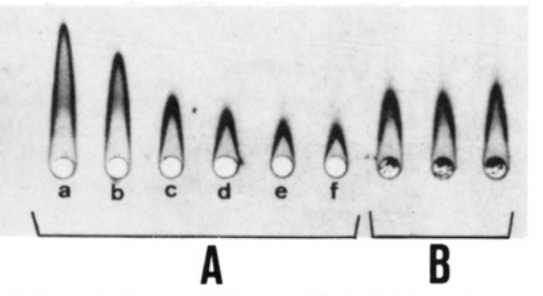


FIGURE 2: Quantitative determination of FABP in heart homogenate by rocket immunology. (A) Purified FABP as standard: (a) 1.98 $\mu$g; (b) 1.32 $\mu$g; (c) 0.99 $\mu$g; (d) 0.79 $\mu$g; (e) 0.66 $\mu$g; (f) 0.56 $\mu$g. Sample volume was 10 $\mu$L in buffer E. (B) FABP detected in supernatant after homogenization (1:40 grams:milliliters) of respectively three rat hearts in buffer E. Sample volume was 10 $\mu$L. Details of the procedure were given under Materials and Methods.

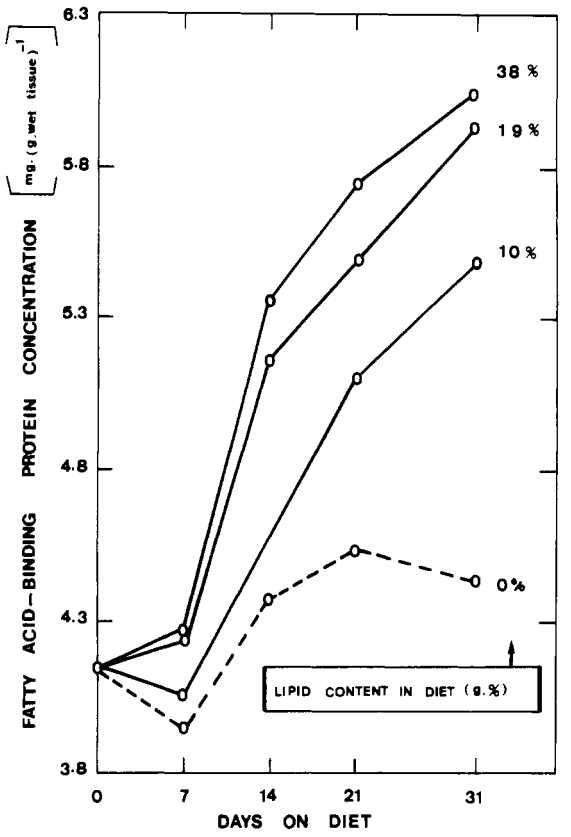


FIGURE 3: Influence of oil content in the diet on cardiac FABP synthesis. Male rats, initially weighing 200 g, were fed ad libitum for 10 days the oil-free $R_0$ diet described in Table I. They were then transferred onto the oil-containing diets $R_{10}$, $R_{19}$, and $R_{38}$ (Table I), respectively, containing 10, 19, and 38 g % of oil (extracted from black currant seeds). All the diets were balanced so that the respective nutrients expressed in milligrams per kilocalories were equivalent, except for oil and starch (Table I). After homogenization of heart tissue, quantitative determination of FABP by rocket immunology was performed according to the description given under Materials and Methods. Each point represents the mean value of three rats.

roborated by two independent experiments in which the oil content of diets was kept constant but the starch or casein content varied strongly. In both cases, FABP concentration remained remarkably constant (results not shown).

In conclusion, the total FABP concentration in the heart is not constant but can be modulated by the oil content of the diet. The mechanism of this induction is far beyond the scope of the present work. However, the biological significance and consequences of this inducibility will be stressed in further parts of this article.

*Subcellular FABP Distribution in Rat Heart.* Following the determination of the physiological FABP concentration in the heart tissue, it became obvious that attribution of specific physiological functions to FABP would be made much easier if we could analyze its intracellular location. Due to the low solubility of long-chain fatty acids in hydrophilic media, a carrier is obviously required for their translocation between the different intracellular compartments. To date, FABP is the best candidate, since it is the only protein found in the heart with a capacity for specifically binding fatty acids. This proposal implies that FABP should be found in all cellular compartments.

In order to obtain a realistic image of the in vivo FABP distribution, a rapid injection of glutaraldehyde into the living heart was performed followed by low-temperature processing of the tissue. Adult male rats weighing 250 g and fed a standard commercial diet (5.6 wt % lipids) were used for this operation. The specific immunocytochemical detection of FABP was then possible, using the elegant protein A–gold particle method.

FABP distribution showed a complex pattern, since the protein was detected in all the heart issue compartments, i.e., the capillary endothelium, the intercellular spaces, and the intracellular compartments such as the myofibrils and the mitochondria (Figure 4). A quantitiative analysis of this distribution was achieved after having taken into account the following considerations. From the work of Anversa et al. (1978), we could calculate that, in the normal adult rat heart, the relative volume occupied by the myocytes is 84.9% (myofibrils, 45.67%; mitochondria, 28.69%; and residual, 10.52%) and the extracellular volume is 15.1% (intercellular spaces, 8.7%; capillary endothelium, 3.2%; capillary lumen, 3.2%). The residual compartment mentioned above is mainly represented by the spaces surrounding the mitochondria. In the present study, the gold particle mean densities, specific to FABP, counted on a total of 60 micrograph fields and located respectively on the myofibrils (myo), the mitochondria (mit), the residual spaces (resid), the intercellular spaces (ics), and the capillary endothelium (endo) were the following: 138 ± 26, 44 ± 10, 55 ± 8, 21 ± 4, and 65 ± 6 gold particles per square decimeter of micrographic surfaces representing fields enlarged 56000×. If we define $C_{myo}$, $C_{mit}$, $C_{resid}$, $C_{ics}$, and $C_{endo}$ as the FABP concentrations in the respective above compartments, then (a) $C_{mit}/C_{myo} = 0.318$, (b) $C_{mit}/C_{resid} = 0.800$, (c) $C_{resid}/C_{myo} = 0.398$, (d) $C_{endo}/C_{myo} = 0.471$, and (e) $C_{ics}/C_{myo} = 0.152$. Taking into account the total concentration of FABP in the heart (4.3 ± 0.23 mg·g$^{-1}$ wet heart), as determined in the preceding section, and also the relative volume of the different compartments, as discussed previously, we can write the following relation: (f) $0.456C_{myo} + 0.286C_{mit} + 0.105C_{resid} + 0.087C_{ics} + 0.032C_{endo} = 4.3$ mg·g$^{-1}$.

After the equations in (a–f) were solved, FABP concentrations were made explicit for the different compartments. The calculated values were respectively $C_{myo} = 6.96$, $C_{mit} = 2.21$, $C_{resid} = 2.77$, $C_{ics} = 1.05$, and $C_{endo} = 3.28$ mg/g of wet tissue.

These results show that the distribution of FABP is highly gradient-like when one cell compartment is compared to the next one. Furthermore, using the above numerical data characterizing the relative volume of the different compartments and the corresponding FABP concentrations, we obtained the following FABP total distribution: 73.9% on the myofibrils, 14.7% in the mitochondria, 6.7% in the spaces surrounding the mitochondria, 2.4% in the capillary endothelium, and 2.1% in the intercellular spaces.

*Control by FABP of Fatty Acid Partition in Isolated Cardiac Mitochondria.* In the preceding section, we observed that the in vivo FABP concentrations in the mitochondria and in the space surrounding the mitochondria were respectively 2.21 and 2.77 mg·mL$^{-1}$; the immediately adjacent myofibril compartment contained 6.96 mg·mL$^{-1}$, which represents about 2.8 times more. Are there important physiological reasons why FABP concentrations in the mitochondria and in the surrounding spaces should be low compared to the high concentration observed in the near-myofibril compartment?

Experiments were designed to answer this question and to see what happened to the fatty acid distribution pattern when the FABP concentration was varied in an in vitro medium containing isolated mitochondria. The timing and design of the experiments are described under Materials and Methods (see β-Oxidation Rate Measurements) but with the modification that CoA and carnitine were omitted to avoid fatty acid

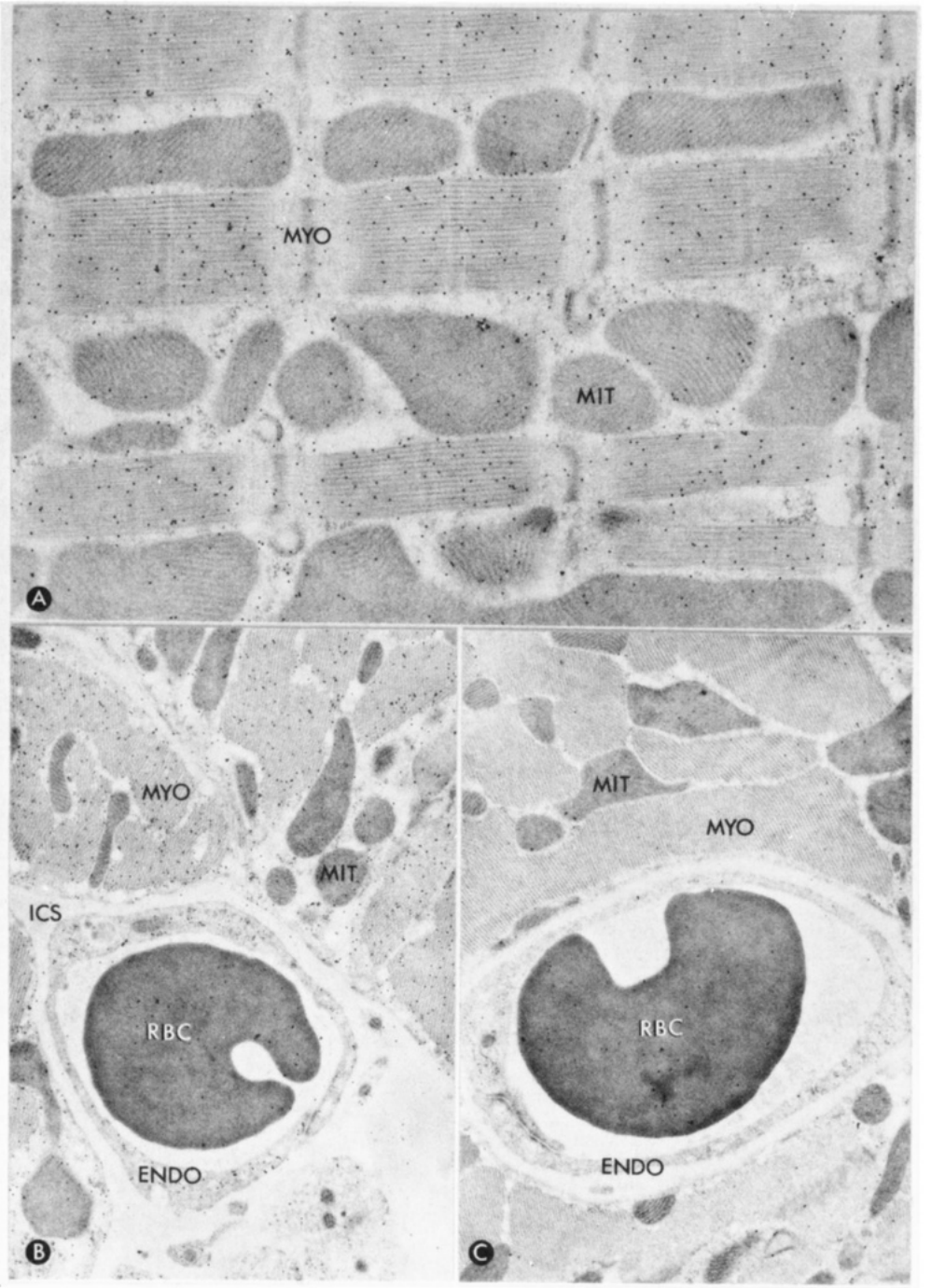


FIGURE 4: Subcellular detection of FABP in rat heart by the immunogold method. Abbreviations: MIT, mitochondria; MYO, myofibrils; ICS, intercellular spaces; ENDO, capillary endothelium; RBC red blood cells. The longitudinal section (A) and the cross section (B) were pretreated with FABP antiserum. The cross section (C) was pretreated with normal rabbit serum and, thus, must be considered as a control sample. The very low background labeling observed in the latter case indicated that the labeling observed in (A) and (B) was very specific to FABP, except on RBC. Enlargements are (A) 18750×, (B) 11250×, and (C) 11250×. Other technical details are given under Materials and Methods.

disappearance by $\beta$-oxidation. The total fatty acid concentration, $A_{tot}$, was kept constant and equal to 15.3 $\mu$M. At equilibrum, fatty acids are expected to be present in the mitochondrial membranes, $A_{in}$, in the surrounding medium, $A_s$, and in specific binding sites, $A_b$, on FABP. This was expressed by the equation:

$$A_{tot} = A_s + A_b + A_{in} = 15.3\ \mu M \qquad (1)$$

In order to proceed to a subsequent mathematical treatment of this system, we needed to quantify the fatty acid equilibrium concentration simultaneously in the three considered compartments: $A_{in}$, $A_b$, and $A_s$. For this purpose, we used the electron spin resonance (ESR) method, by introducing in the system the spin-labeled 12-doxylstearate as a fatty acid. The ESR signal of this label, when moving isotropically and free in the medium, was characterized by three resonance lines: $h_{+1}$, $h_0$, and $h_{-1}$ (Figure 5). The motion of the label was restricted after binding to FABP or to the mitochondrial membranes. Conspicuous modifications of the signal appeared with a concomitant enlargement of the central line width (Figure 5). It is well-known that the height of the high-field line, $h_{-1}$, is proportional to the $A_s$ equilibrium concentration of 12-doxylstearate free in the medium. This value can be determined by comparison with a sample containing a known

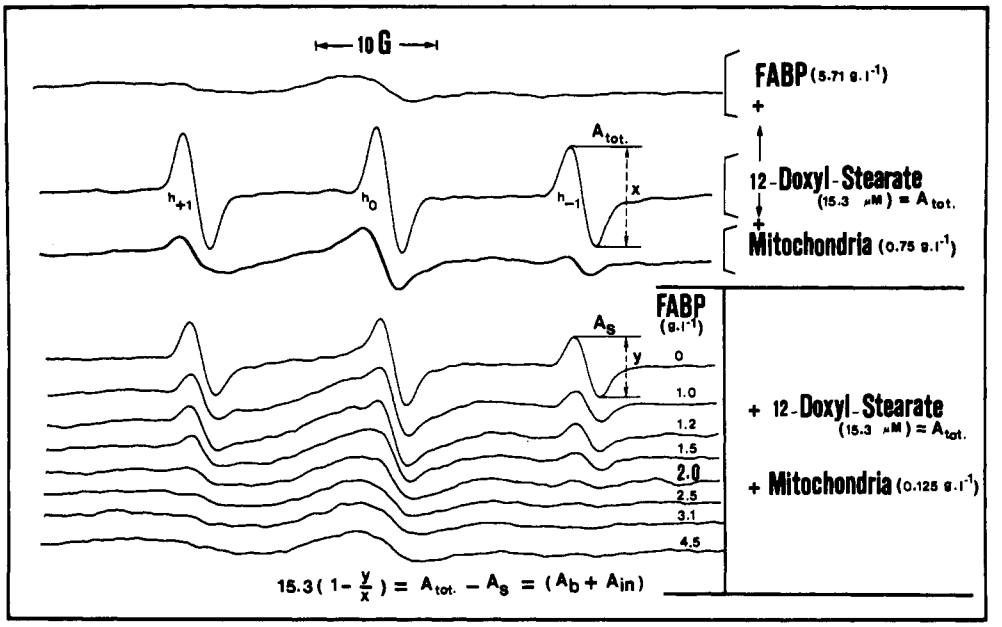


FIGURE 5: Binding of 12-doxylstearate to FABP and to mitochondrial membranes as visualized by electron spin resonance (ESR). Purified FABP, 12-doxylstearate, isolated mitochondria, and required cofactors (but omitting CoA and L-carnitine) were mixed in buffer C as described under Materials and Methods (see β-Oxidation Rate Measurements). After 1.5-min equilibration at 37 °C, ESR signals were recorded. 12-Doxylstearate (final concentration $A_{tot}$ = 15.3 μM) was partitioned between the mitochondrial membranes ($A_{in}$), the external medium ($A_s$), and the binding sites ($A_b$) on FABP. Equilibrium concentrations in these compartments were then determined as detailed under Results and as visualized in Figures 6, 7, and 8a.

Table II: Numerical Values of the Parameters $K_i$, $n_i$, $\bar{V}_{i,max}$, and $C$ in Equations 2–4[a]

| parameters | value | SD of parameter estimates |
|---|---|---|
| $\bar{V}_{max_{II}}$ | 3.48[b] | 0.48 |
| $\bar{V}_{max_{III}}$ | 10.93[b] | 0.62 |
| $K_1$ | 0.88[c] | 0.38 |
| $C$ | 0.84[c] | 0.39 |
| $K_2$ | 5.34[d] | 0.15 |
| $K_3$ | 1.00[d] | 0.14 |
| $n_1$ | 3.21[e] | 0.99 |
| $n_2$ | 15.39[e] | 6.91 |
| $n_3$ | 1.00[e] | 0 |

[a] Numerical values were determined by nonlinear regression (Gauss–Newton algorithm) from the experimental points of Figures 6 and 7. The significance of parameters has been detailed under Results. [b] μM·g⁻¹. [c] g·L⁻¹. [d] μM·L⁻¹. [e] Dimensionless.

standard quantity of label. This method of quantitative comparisons has been justified and explained in detail in a previous publication (Fournier et al., 1983). After consideration of the spectra and symbols in Figure 5, the experimental $A_s$ and $A_{in}$ + $A_b$ values can be determined easily, since

$$A_s = A_{tot}Y/X = 15.3Y/X$$

$$A_{in} + A_b = A_{tot} - A_s = 15.3[(X - Y)/X]$$

The variations of these two experimental quantities, $A_s$ and $A_{in}$ + $A_b$, as a function of $P$, which represents the FABP concentration, have been mathematically analyzed by using nonlinear regression techniques. The best representation of the experimental points was obtained (Figure 6) when the following sigmoidal curves were considered:

$$A_s = \frac{A_{tot}}{1 + [(P + C)/K_1]^{n_1}} \quad (2)$$

$$A_{in} + A_b = \frac{A_{tot}}{1 + [K_1/(P + C)]^{n_1}} \quad (3)$$

$K_1$ defines the point of half-saturation of the curves (the $P$ + $C$ value at which $A_s = A_{tot}/2$ and $A_{in} + A_b = A_{tot}/2$); $n_1$ is

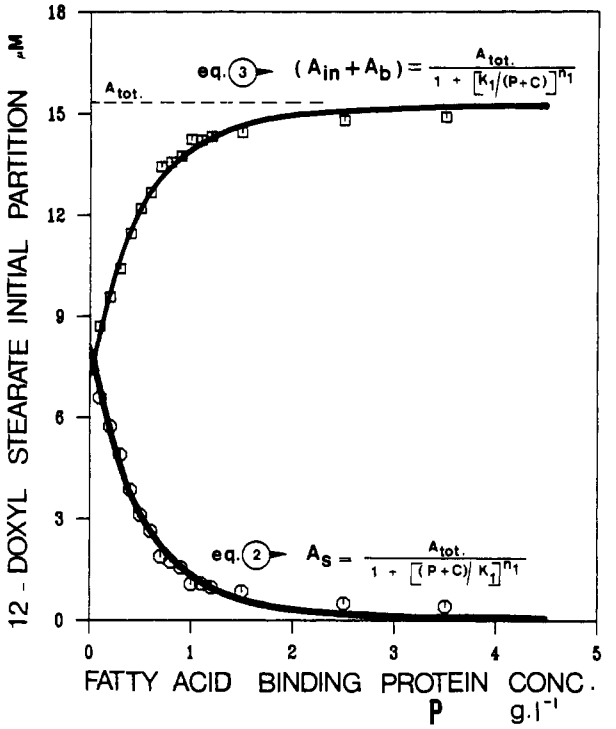


FIGURE 6: Equilibrium distribution of 12-doxylstearate in isolated mitochondria as a function of FABP concentration. Equilibrium concentrations of 12-doxylstearate in the mitochondrial membrane ($A_{in}$) and the external medium ($A_s$) and that bound to FABP ($A_b$) were obtained by ESR spectroscopy (Figure 5) and calculated according to the procedure detailed under Results. The two fitted curves were obtained by applying a nonlinear least-squares method to the experimental points, using the theoretical sigmoidal-type equations, eq 2 and 3. The numerical values of the estimated parameters are listed in Table II.

an adjustable parameter defining the sigmoidal character of the curves; $C$ is a constant such that $A_s = A_{tot}$ = 15.3 μM, and $A_{in}$ + $A_b$ = 0, when $P = -C$. These parameters and their statistical variations have been reported in Table II. The

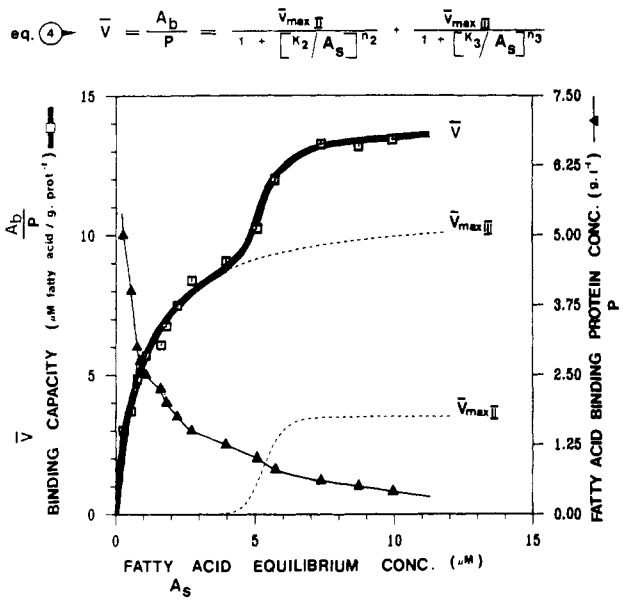


FIGURE 7: Binding capacity of 12-doxylstearate to FABP. Mixing and equilibrating 12-doxylstearate with variable FABP concentrations and required cofactors in buffer C, at 37 °C, were as described under Materials and Methods (see β-Oxidation Rate Measurements), but omitting the mitochondria. ESR spectra obtained for the different FABP concentrations, $P$, were analyzed quantitatively as detailed under Results. The solid line represents the predicted binding curve according to eq 4 and the parameters of Table II and fitted to the experimental points which are represented by squares. The dashed lines represent the computer deconvolution of the complex binding curve $\bar{V}$ into a hyerbolic and a sigmoidal curve, respectively, characterized by the maximal binding capacity $\bar{V}_{max_{III}}$ and $\bar{V}_{max_{II}}$.

excellent fit of both curves to the experimental points is obvious when we consider their graphic expression in Figure 6.

In order to obtain explicit values of the three variables $A_{in}$, $A_b$, and $A_s$ as a function of FABP concentration, $P$, one more equation was required. For this purpose, quantitative values of $A_b$, as a function of $P$, have been determined by using the same ESR methodology as described above. However, the mitochondria were omitted in the reaction mixture. The isotherm representing the variations $A_b/P$ as a function of $A_s$ was complex (Figure 7). It was deconvoluted into a hyperbolic plus a sigmoidal curve (Figure 7). The sum of these two components has been symbolized by the equation:

$$\bar{V} = A_b/P = \frac{\bar{V}_{max_{II}}}{1 + (K_2/A_s)^{n_2}} + \frac{\bar{V}_{max_{III}}}{1 + (K_3/A_s)^{n_3}} \quad (4)$$

$\bar{V}_{max_{II}}$ and $\bar{V}_{max_{III}}$ represent the maximum binding capacity of fatty acid to protein in the sigmoidal and the hyperbolic part of the curve, respectively (Figure 7); $K_i$ values are the points of half-saturation of the curves (the $A_s$ value at which $\bar{V} = \bar{V}_{max}/2$); $n_i$ values are adjustable parameters defining the sigmoidal character of the curves and are related to the fatty acid concentration corresponding to the inflection point, $A_{si}$, according to the relation

$$A_{si} = K_i[(n_i - 1)/(n_i + 1)]^{1/n_i}$$

which can be obtained by solving

$$d^2\bar{V}_i/dA_s^2 = 0$$

$\bar{V}_{i,max}$, $K_i$, and $n_i$ parameters in eq 4 were estimated from the experimental points of Figure 7 by using a nonlinear least-squares technique. The numerical values are listed in Table II, and the fitted curve is shown in Figure 7.

The complex shape of this binding isotherm is due to the coexistence of multispecies of FABP, by self-aggreation, as

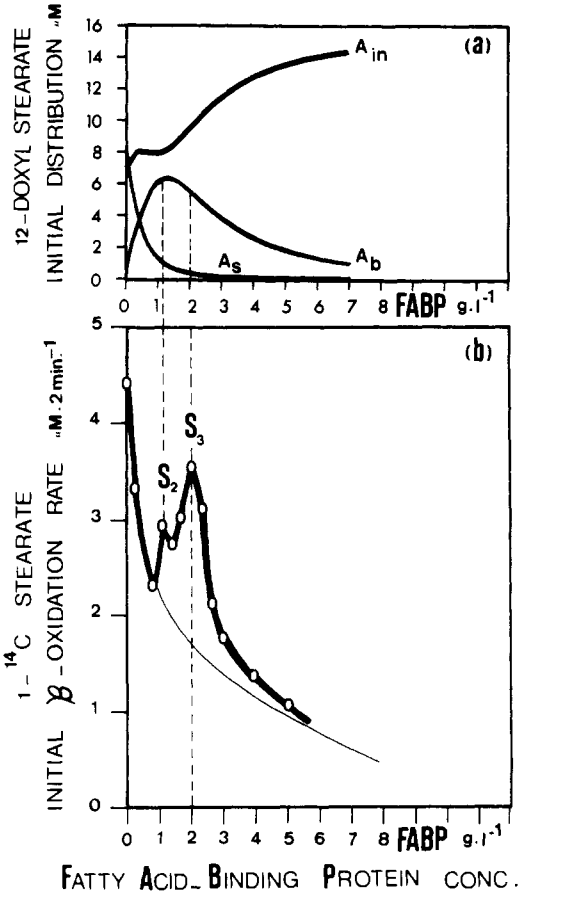


FIGURE 8: (a) Influence of FABP on the equilibrium partition of spin-labeled 12-doxylstearate in isolated mitochondria. Equilibrium concentrations of 12-doxylstearate at 37 °C in mitochondrial membranes ($A_{in}$) and in the external medium ($A_s$) and that bound ($A_b$) to FABP were obtained by computer-assisted resolution of the phenomenological equations, eq 1–4 (see Results). The experimental values required for the resolution of this equation system were obtained as described in Figures 5–7 and Table II. (b) Control by FABP of [1-$^{14}$C]stearate β-oxidation rate in isolated mitochondria. Mixing and preequilibration of [1-$^{14}$C]stearate plus stearate (final concentration 15.3 μM), purified FABP, isolated cardiac mitochondria, and required cofactors in buffer C were as detailed under Materials and Methods. After 2-min incubation at 37 °C, the samples were saponified and fatty acid extracted. Fatty acid β-oxidation rates were obtained by comparing the radioactivity value remaining in the test sample with the value of a nonincubated control sample.

we demonatrated in two previous publications (Fournier et al., 1983; Fournier & Rahim, 1983). The phenomenological equations (eq 1–4) relating the three unknown quantities, $A_{in}$, $A_s$, and $A_b$, to FABP concentrations in the medium explicitly described the above equilibrium system. Mathematical resolution of these equations by computerization yielded the simultaneous equilibrium values of these quantities, as represented in Figure 8a.

As a first general observation, we can see that variations of FABP concentrations induced dramatic changes of fatty acid distribution in the three considered compartments (Figure 8a). $A_s$ values were constantly decreasing, whereas $A_{in}$ values were constantly increasing. $A_b$ variations were quite remarkable, since for FABP concentrations ranging between 1 and 3 mg·mL$^{-1}$ the curve shows a maximum (Figure 8a). This maximum is well correlated with the in vivo FABP concentrations observed in the mitochondria and in the residual space surrounding the mitochondria, i.e., 2.21 and 2.77 mg·mL$^{-1}$, respectively.

*Control by FABP of Fatty Acid Catabolism in Isolated Heart Mitochondria.* The mitochondrial β-oxidative system,

comprising the acyl-CoA activation and acylcarnitine transmembrane transport, plus the matrix β-oxidative enzymes, is the most important source of energy in the heart, since it produces about 80% of cardiac energy. Which of the three previously discussed pools, $A_s$, $A_b$, or $A_{in}$, provides fatty acids as a fuel for this mitochondrial system will be investigated in this section. It is obvious that FABP, via the control exerted on the fatty acid content in these three pools (Figure 8a), is expected to be an important parameter regulating the energy output of the β-oxidative system.

Purified FABP, isolated mitochondria, [1-$^{14}$C]stearate, and the required cofactors were mixed in vitro. The experimental scheme was designed in such a way that preequilibration of all the components took place before the start of the reaction, which was induced by the concomitant arrival of CoA and carnitine in the incubation medium. The rate of stearate β-oxidation obtained after 2 min of incubation at 37 °C was observed to be strongly dependent upon FABP concentration (Figure 8b). A general depression of the rate was induced by increasing FABP concentrations. However, two very remarkable peaks of activity, superimposed on this depressed curve, were observed for FABP concentrations between 1 and 3 mg·mL$^{-1}$ (Figure 8b).

From the above observations, we can conclude that the membrane-linked fatty acid pool, $A_{in}$, was not correlated with the β-oxidation rate. The former was increasing when the latter was decreasing (Figure 8a,b). Consequently, it can be excluded as a pool providing fatty acids to the β-oxidative system.

The $A_s$ pool (fatty acid free in the medium) was able to deliver fatty acid to the β-oxidation system; a good correlation was observed between the two events for FABP concentrations between 0 and 1 mg·mL$^{-1}$; both curves were decreasing in this range (Figure 8a,b).

The $A_b$ pool, representing fatty acid bound to FABP, was obviously the fatty acid supplier to the β-oxidative system for FABP concentrations between 1 and 3 mg·mL$^{-1}$. In fact, an excellent correlation between the maximum fatty acid content, $A_b$, on FABP (Figure 8a) and the β-oxidation rate (Figure 8b) was observed in this FABP concentration range. Remarkably, mitochondrial and perimitochondrial in vivo FABP concentrations were shown to be also in this concentration range.

## Discussion

In normal, well-oxygenated hearts, fatty acids have been identified many years ago in both in vivo and in vitro studies to the preferred substrate for energy generation (Neely et al., 1972). However, this organ is a poor fatty acid synthesizer and is thus strongly dependent upon circulating lipids as a source of fatty acids. How this fuel is transported from the blood capillaries to the mitochondrial matrix in the core of the cell in order to be catabolized by β-oxidation remains a problem to be solved. Albumin, a well-known fatty acid carrier, was recently shown to be present in the heart not only in the blood vessels but also in the intermyocyte spaces and their cellular prolongations, i.e., in the T tubules (Yokota, 1982). Consequently, this carrier is a good candidate for the translocation of fatty acids from the bloodstream to the cell membrane of myocytes. However, albumin being absent inside the cells, the question remains how fatty acids are translocated from the cellular membrane to the intracellular organelles using them, such as the mitochondria or the endoplasmic reticulum. The pertinence of this question is stressed by the fact that preferentially long-chain fatty acids, sparingly soluble in the cytoplasm and therefore requiring a carrier, are used as a fuel by the mitochondria. An excellent candidate which would be able to serve as a specific intracellular transporter for fatty acids is suggested by our work (Fournier et al., 1978, 1983; Fournier & Rahim, 1983) on a cardiac protein which is able to bind fatty acids and thus named fatty acid binding protein (FABP).

The aim of our study was, first of all, the development of an efficient new method for the purification of this protein (Figure 1), its quantification by immunorocket electrophoresis (Figure 2), and its subcellular detection in vivo by the protein A–gold particle method (Figure 4). The protein was detected in the capillary endothelium (3.28 mg·mL$^{-1}$), in the intercellular spaces (1.05 mg·mL$^{-1}$), and (remarkably according to a gradient-like pattern in the myocytes) on the myofibrils (6.96 mg·mL$^{-1}$), in the perimitochondrial spaces (2.77 mg·mL$^{-1}$), and in the mitochondria (2.21 mg·mL$^{-1}$). The ubiquity of this protein in all the heart cell compartments is an excellent argument for the presumed fatty acid carrier function of FABP.

In addition to this carrier function, a second function for FABP, as a fatty acid supplier to the mitochondrial β-oxidative system, was also anticipated because of the location of the protein detected inside and close to the mitochondria (Figure 4). An experimental model involving a fixed concentration of isolated cardiac mitochondria and stearic acid, but variable concentrations of FABP, was elaborated and aimed at studying the influences of FABP upon the rate of fatty acid catabolism in isolated mitochondria. In fact, FABP acts as a powerful regulator of the β-oxidative system. A remarkable FABP-dependent activity profile was observed characterized by two peaks of fatty acid β-oxidation activity at FABP concentrations between 1 and 3 mg·mL$^{-1}$ (Figure 8b). On both sides of this concentration range, mitochondrial β-oxidative activity falls monotonously as the concentration of FABP increases.

This regulation of the β-oxidative system by FABP is very efficient when one considers that small FABP concentration variations in the physiological range (1–3 mg·mL$^{-1}$) are sufficient to strongly modify β-oxidative activity (Figure 8b). This potential regulation of mitochondrial energy production by FABP obviously would be physiological only if the concentration of FABP is able to temporally fluctuate inside or close to the mitochondria. Such requisite fluctuations are likely to occur in vivo. In fact, there is evidence that such local variations might exist.

One of the possible inducing factors leading to long-term fluctuation of FABP gradients in the cells might be the diet. We observed that the oil content in the diet conspicuously increased the total FABP of the heart. After 31 days on a diet containing 10%, 19%, or 38% oil, increases of FABP of 32%, 42.8%, and 45%, respectively, were observed in rat heart compared to a diet lacking in oil (Figure 3).

Intermediate-term variations of the gradient distribution also seem likely if one considers that the total cardiac FABP varies rhythmically in the course of a day. The synthesis in the nocturnal phase is higher than that in the diurnal phase (Glatz et al., 1984).

In the short term, rapid fluctuations of these gradients are also conceivable. The heart is a muscle of constant mechanical activity going through contraction–relaxation cycles of the myofibrils. Every cycle is probably followed by a brief period of mixing in the intracellular pools and compartments. As a consequence of this mixing, the FABP concentration could fluctuate in and around the mitochondria. The result would be a periodic FABP-dependent flux of fatty acid reaching the mitochondrial β-oxidative enzymes. This rhythmic flux might as a result generate an equally rhythmic output of energy.

The next step in this study was aimed at elucidating the mechanism of this control exerted by FABP on the β-oxidative system. The latter is very complex since enzymatic transformations of fatty acid into acyl-CoA and transmembrane migratory processes of acylcarnitine through the inner mitochondrial membrane are required before final enzymatic β-oxidation in the matrix. However, as a preliminary process preceding this complex biochemical cascade of events, it is obvious that partitioning of fatty acid must occur between the mitochondrial membranes ($A_{in}$), the binding sites ($A_b$) on FABP, and the surrounding cytoplasmic medium ($A_s$). This partitioning, as a key step before the subsequent fatty acid β-oxidation, was shown in the present study to be under the direct control of FABP. To investigate this, we used the electron spin resonance technique and spin-labeled stearic acid for the determination of equilibrium concentrations of fatty acid between these three compartments (Figure 5). Correlation analysis of the initial equilibrium fatty acid concentration with the initial fatty acid β-oxidation rate, as a function of FABP concentration, indicates that fatty acid bound to FABP, $A_b$, obviously is the source of substrate for the β-oxidative system. The maximal fatty acid content in this pool is well correlated with the maximal fatty acid β-oxidation rates (Figure 8a,b). The two correlated events were observed to be maximal at FABP concentrations between 1 and 3 mg·mL$^{-1}$. Remarkably, this active in vitro range is the same as the in vivo FABP concentration range observed in the mitochondria (2.21 mg·mL$^{-1}$) and in the perimitochondrial spaces (2.77 mg·mL$^{-1}$). The physiological FABP concentration naturally occurring in vivo in the mitochondria and in the immediate surrounding spaces was thus selected by nature in this optimized concentration range in order to maximize the fatty acid transferable as a substrate to the β-oxidative system.

The determination of the FABP-dependent fatty acid distribution as described above is the result of mathematical computations based on the phenomenological equations, eq 2–4. These equations excellently describe the fatty acid binding curves to FABP and to mitochondria (Figures 6 and 7), but due to their phenomenological nature, they do not explain why both fatty acid binding to FABP and fatty acid β-oxidation rates are correlated and maximal at FABP concentrations between 1 and 3 mg·mL$^{-1}$ (Figure 8a,b). However, in our previous publication concerning the molecular self-aggregation properties of FABP (Fournier et al., 1983), it was demonstrated that in this concentration range at least three different self-aggregated FABP species were coexisting at equilibrium. Furthermore, the high molecular weight species was shown to be less capable of binding to fatty acid compared to the low molecular weight species (Fournier & Rahim, 1983). This differential binding capacity, as a function of the aggregation state of the protein, is the rational basis explaining the bell-shaped curve of fatty acid binding to FABP as shown in Figure 8a and the concomitant evolution of β-oxidation rates (Figure 8b). At FABP concentrations beyond 3 mg·mL$^{-1}$, the high molecular weight self-aggregated FABP species exists almost exclusively and with a low affinity for fatty acids. Thus, the binding curve (Figure 8a) and concomitantly the β-oxidation rates, driven by the fatty acid bound to FABP, dramatically drop (Figure 8b). In the FABP concentration range between 1 and 3 mg·mL$^{-1}$ mostly, low molecular weight self-aggregated FABP species are coexisting, but with a high affinity for fatty acids. This is the reason why both the binding curve and the β-oxidation rates depending upon this bound fatty acid go through maximal values in this concentration range (Figure 8a,b). This direct correlation between the fatty acid binding to FABP and the β-oxidation rates, as a function of FABP concentration, suggests that the two β-oxidative peaks observed in this critical FABP concentration range of 1–3 mg·mL$^{-1}$ (Figure 8b) are due to the transfer of fatty acids from the FABP pool toward the mitochondrial β-oxidative system, but are specifically driven by only two of the three self-aggregated FABP species. Local concentration variations of FABP in the mitochondrial vicinity are expected to modify the equilibrium concentrations of these two active species and consequently the energetic output of the β-oxidative system.

The biophysical or biochemical steps specifically controlled by these two active FABP species remain to be investigated. However, it is likely that both the fatty acid transfer from the cytoplasm to the outer mitochondrial membrane-linked enzyme, acyl-CoA synthetase, and the subsequent acyl-CoA transfer to the inner membrane enzyme, acylcarnitine transferase, might well be the FABP-dependent processes.

The central emerging idea of the present study delineates the self-aggregation capacity of the cardiac fatty acid binding protein (FABP) and its in vivo gradient-like distribution as new and important parameters in the regulation of the mitochondrial β-oxidative system, the pathway providing 80% of the energy required by the heart.

## ACKNOWLEDGMENTS

We are grateful to M. Beaud for her high-quality art in electron micrograph reproduction, to W. Jaggi for the maintenance of animals, to J. J. Pahud for his help in rabbit immunization, and to L. Arimanana for his technical assistance in heart perfusion. We also thank D. Farr, M. Horisberger, and H. Hottinger for their comments and help in editing of the text.

**Registry No.** Stearic acid, 57-11-4.

## REFERENCES

Anversa, P., Loud, A. V., Giacomelli, F., & Wiener, J. (1978) *Lab. Invest. 38* (*5*), 597–609.

Carlemalm, E. (1982) *Instructions for Use of Lowicryl K4M and HM20*, Biozentrum, University of Basel, Switzerland.

Fournier, N. C., & Rahim, M. H. (1983) *J. Biol. Chem. 258*, 2929–2933.

Fournier, N., Geoffroy, M., & Deshusses, J. (1978) *Biochim. Biophys. Acta 533*, 457–464.

Fournier, N. C., Zuker, M., Williams, R. E., & Smith, I. C. P. (1983) *Biochemistry 22*, 1863–1872.

Glatz, J. F. C., Baerwaldt, C. C. F., Veerkamp, J. H., & Kempen, H. J. M. (1984) *J. Biol. Chem. 259*, 4295–4300.

Gogstad, G. O., & Krutnes, M. B. (1982) *Anal. Biochem. 126*, 335–359.

Hsia, J. C., Wong, L. T. C., & Kalow, W. (1973) *J. Immunol. Methods 3*, 17–24.

Kellenberger, E., Carlemalm, E., Villiger, W., Roth, J., & Garavito, R. M. in *Low Denaturation Embedding for Electron Microscopy of Thin Sections*, Chemische Werke Lowi GmbH, Waldkraiburg, West Germany.

Morton, R. K. (1955) *Methods Enzymol. 1*, 45.

Neely, J. R., Rovetto, M. J., & Oram, J. F. (1972) *Prog. Cardiovasc. Dis. 15*, 289–329.

Ockner, R. K., Manning, J. A., Popenhausen, R. B., & Ho, W. K. L. (1972) *Science* (*Washington, D.C.*) *177*, 56–58.

Pharmacia Fine Chemicals Brochure (1982) *Isoelectric Focusing, Principles and Methods*, p 86, Uppsala, Sweden.

Reynolds, E. S. (1963) *J. Cell Biol. 17*, 208–213.

Yokota, S. (1982) *Histochemistry 74*, 379–386.